32nd URSI GASS, Montreal, 19-26 August 2017

Multi-band Multi-beam Performance Evaluation of On-Site Coding Digital Beamformer using Ultra-Wideband Antenna Array

Satheesh Bojja Venkatakrishnan*(1), Elias A. Alwan(1), and John L. Volakis(1)
(1) The Ohio State University, Columbus, Ohio, 43210
email: bojjavenkatakrishnan.1@osu.edu

Abstract

Cognitive and software defined radios require ultra-wideband (UWB) antennas with digital beamforming. Recently, a novel on-site coding receiver (OSCR) architecture was proposed to significantly reduce hardware requirement for digital beamforming. At the receiver side, we propose to code several antenna outputs in the analog domain prior to digitizing them using a single analog-to-digital converter (ADC). Decoding will be done using field programmable gate arrays (FPGA) in the digital domain to perform beamforming. Doing so, hardware requirements are drastically reduced. In this paper, we demonstrate the validation of the OSCR concept by building and testing a multi-band multi-beam receiver. Measurements are performed in an anechoic chamber using an UWB antenna array operating from 200MHz - 2.5GHz, for two transmit signals modulated at f_1 and f_2, and incident on the receiver from various angles. Results show an accurate estimate of the angle of arrival, proving that on-site coding can perform with minimal or no degradation in signal-to-noise ratio (SNR) in a multi-beam and multi-band environment.

1. Introduction

Future wireless communication systems will require increasingly higher data rates. This compels the realization of high speed communication system using a single multi-functional front-end (transceiver) integrated into an ultra-wideband (UWB) aperture. Multi-channel transceiver combined with UWB antenna array, provides digital beamforming capability, thus overcoming the inherent pathloss incurred by any RF system. Indeed, digital beamforming will improve the signal to noise ratio (SNR) and spatial diversity by rejecting interference from unwanted beam directions. Recently, tightly-coupled UWB antenna arrays were proposed with bandwidths > 10:1 [1-4]. The overall challenge is to design a digital back-end with advanced signal processing capability to achieve spatial filtering, high gain, high interference mitigation, and reliability across wide bandwidth. As recent advances in digital technology and signal processing has led to reduced complexity, these challenges are within our reach.

Conventional RF beamformers are based on true time delay (TTD) and analog phase shifters [5]. Besides, analog phase shifters have limited phase tuning and can only handle a single spatial direction at a time. In addition to complex hardware requirements, they also suffer from phase errors, resolution and small bandwidths. These limitations can be overcome by implementing beamforming in the digital domain [6-8]. However, a drawback for current digital beamformer is the complex RF and analog circuitry at the analog front-end that must be repeated for each antenna receiver element. This approach leads to increased cost, large form factor and excessive power consumption. The latter is proportional to the analog-to-digital converters (ADCs) in the receiver.

It is necessary to reduce the number of ADCs for power consumption reduction. Indeed, the need for hardware reduction and wide bandwidth in RF systems led to the OSCR presented in [9-12]. This scheme employs code division multiplexing (CDM), depicted in Fig. 1. The proposed OSCR architecture allows for full control of the phase at each array element/path. Further, it provides significant reduction in cost, area, power and hardware requirements, making it an attractive option for handheld beamforming applications.

In this paper, for the first time, we carry out multi-band multi-beam validation and evaluation of a multi-channel OSCR in an anechoic chamber. Specifically, two different signals are transmitted at two frequencies (f_1 and f_2) simultaneously from various locations. Using an 8-channel OSCR, we estimate the direction of arrival of the incoming wave and recover the transmitted signal with minimal SNR degradation.

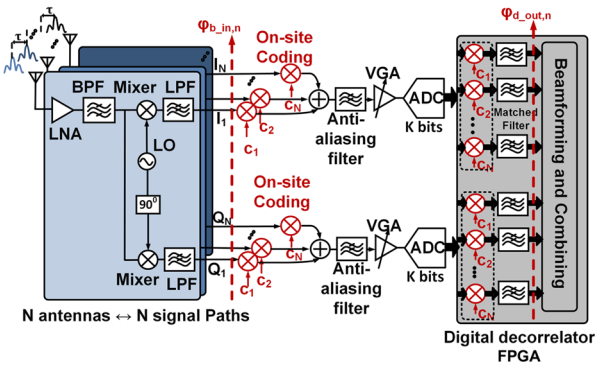

Figure 1. Proposed on-site coding digital beamformer

2. On-Site Coding Receiver Architecture

The proposed novel digital beamforming OSCR architecture is depicted in Fig. 1. Using OSCR, the signal from each antenna element is encoded, then several of these signals are grouped and digitized using a single analog-to-digital converter (ADC). At the digital back-end, field programmable gate arrays (FPGA) are used to decorrelate and recover the signals associated with each array element for beamforming. Doing so, hardware requirements are drastically reduced.

The RF front-end of the proposed OSCR, depicted in Fig. 1, houses a low noise amplifier (LNA), and bandpass filters (BPF) to remove undesired harmonics and interference. Also, as usual, a mixer, and a local oscillator are used to downconvert the modulated signal received by each antenna element to baseband. At baseband, the signal is decomposed into in-phase (I) and quadrature phase (Q) components. A lowpass filter (LPF) is also used to remove high frequency noise. Upon extraction of the I/Q signal, encoding is carried out by multiplying each array element signal with unique orthogonal codes generated by the FPGA. As a result of coding, the baseband signal bandwidth is $BW_{code} = L_c \times B$, where L_c is the length of the spreading code, C_i, and B is the signal bandwidth. The encoded baseband signals, each of bandwidth BW_{code} is subsequently combined vectorially for digitization.

In the digital back-end, the combined I/Q signals (already digitized) are decorrelated. This involves decoding and matched filtering to recover the original signals. To decode after digitization using a single ADC, the signal is first multiplied by the same orthogonal codes to recover the original baseband signal. Because of their unique orthogonality, these signals are readily associated with the array elements receiving them. The decoded signal is then filtered to reduce the quantization noise effects. Finally, phase information φ_i is extracted using

$$\varphi_i[n] = tan^{-1}\left(\frac{Q_{i,dec}[n]}{I_{i,dec}[n]}\right) \quad (1)$$

With the information from the computed phase, we next find the respective delays along each array path and estimate the angle of arrival using

$$\theta_s = sin^{-1}\left(\frac{\lambda \Delta\varphi_{ij}}{2\pi d_{ij}}\right) \quad (2)$$

In the above, λ is the wavelength corresponding to the frequency of operation, $\Delta\varphi_{ij}$ corresponds to the phase difference between the ith and j^{th} path estimated using (1), and d_{ij} is the antenna element spacing between them. After computing the phase of the recovered baseband signals, we apply suitable weights and compute the delays to the signals in each path. Having these, we can coherently combine them into a single path and perform digital beamforming.

3. OSCR with 8-Channel - Hardware Implementation

For the first time, an 8-channel experiment of this complexity is performed to characterize the efficiency of on-site coding. Dual-band measurements were performed simultaneously using 2 transmitters to emulate two simultaneous beams. The test setup is shown in Fig. 2. In this case, only SNR and phase error parameters were evaluated. The performance of OSCR was evaluated by performing angle of arrival measurements in anechoic chamber.

For this evaluation, an UWB antenna array was used as a receiving antenna to test the OSCR's back-end architecture at different frequencies simultaneously. Namely, we tested at 1350MHz (f_1) and 1800MHz (f_2). A dual polarized tightly coupled dipole array with integrated feed network operating in the 200MHz - 2.5GHz frequency range was used as the receiver array. Specifically, the resistive sheet (R-Card), eliminates the mid-band resonance when the dipole-groundplane distance becomes <λ/2. Doing so, a 13.9:1 infinite-array impedance-matching bandwidth with VSWR<2.6 was achieved [4].

Two separate RF boards, acting as transmitters, convert the two-uncorrelated bit sequence to analog signal using digital-to-analog convertor (DAC). The signals were also pulse-shaped using a root-raised cosine (RRC) filter to limit spectral bandwidth to 3.6MHz. This prevented inter-symbol-interference (ISI) prior to conversion. The employed modulation was quadrature phase shift keying (QPSK), and the signals were filtered and up-converted to two different frequencies using an inbuilt oscillator. The modulated signals were then amplified using PAs and transmitted via two horn antennas.

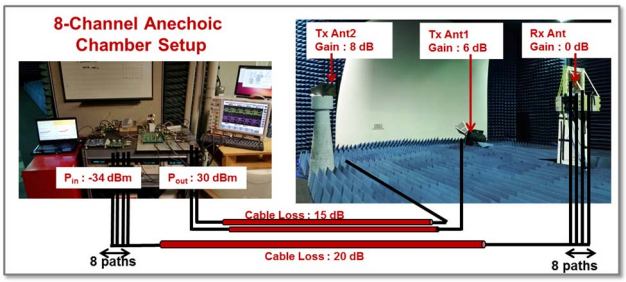

Figure 2. (Left Image) Receiver section on the workstation showing the 8-channel OSCR, (Right Image) Antenna location in anechoic chamber used for measurement

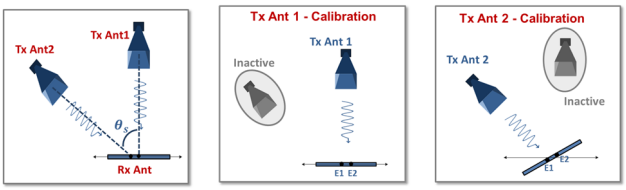

(a) (b) (c)

Figure 3. (a) Block diagram of the actual setup with two transmit antenna, (b) Setup when Transmit Antenna 1 excited while Transmit Antenna 2 is inactive, and (c) Setup when Transmit Antenna 2 excited while Transmit Antenna 1 is inactive.

At the receiver, the elements of the antenna array were connected directly to 8 RF boards using low loss phase matched cables. These RF boards were used as receivers to downconvert the incoming signals into baseband. Using OSCR, the baseband I/Q signals were then encoded using a custom-built encoder board (OSCR board). The orthogonal codes were generated using the FPGA, and used to encode the I/Q signals. These were subsequently combined and digitized using a single dual-channel ADC with 14-bit resolution and sampling at 256MSPS. It should be noted that a single ADC was employed for the entire OSCR experiment communication system. The digitized signal was then fed to FPGAs for further post-processing and beamforming.

4. Anechoic Chamber Setup

To fully exploit the UWB features of the employed antenna array and OSCR receiver, we carried out measurements in the anechoic chamber using 8 RF receiver boards. The measurement setup of the transmit and receive antennas in the anechoic chamber is shown in Fig. 2. The measurement array was mounted on a rotating column for azimuth rotation. The OSCR digital back-end was then placed on the workstation outside the chamber, as shown in Fig. 2.

The experiment involves the angle of arrival estimation from two transmit horns at different locations. The locations of the 2 transmit horns are depicted in Fig. 2. The first transmit horn antenna (Tx Ant 1) is located at boresight with reference to the receiver antenna and is used for calibration. However, the location of the second transmit horn antenna (Tx Ant 2) is at unknown angle θ_s and needs to be determined, as shown in Fig. 3(a).

For testing, a single tone signal at frequency 1800MHz was transmitted using Tx Ant 1, while Tx Ant 2 was inactive and the receiving array was rotated along the azimuth plane (see Fig. 3b). Another single tone was also transmitted using Tx Ant 2 while Tx Ant 1 was inactive, (see Fig. 3(c)). In both cases, two receiving antenna elements (E1 and E2, shown in Fig. 3(b)) were symmetrically placed with reference to the center of the array. Using the captured signals and (2), θ_s was computed. This θ_s corresponds to the Tx Ant2 location. For this experiment, the location of Tx Ant 2 with reference to the normal of the receiver antenna, was estimated to be 49.46^0.

5. Measurements and Results

After finding the locations of the transmit antennas, multi-band/multi-beam measurements were performed in anechoic chamber using 8-channels with the setup shown in Fig. 2. The measurement in the anechoic chamber included five different test cases, namely $\{\theta_{s1}, \theta_{s2}\}$= $\{0^0, 50^0\}$, $\{10^0, 40^0\}$, $\{20^0, 30^0\}$, $\{-30^0, 20^0\}$, and $\{-40^0, 10^0\}$ for frequency band f_1 = 1350MHz and f_2 = 1800MHz. In other words, dual beams from 5 different locations were incident on the receiver antenna simultaneously. The incident angles were also altered by mechanically rotating the receiver antenna array on a foam column, precisely controlled using a servo motors with 0.1^0 accuracy.

At the antenna array, signals were received, down-converted to baseband and filtered using RF boards. The baseband I/Q signal were then encoded using WH codes generated by the FPGA, and combined for digitization using a single dual-channel ADC. In the FPGA, signals were decorrelated, and the phase was computed using (1) followed by the angle of arrival estimation using (2).

Table 1 shows the incident (θ_{S_j}) and decoded angles ($\hat{\theta}_{S_j}$) for various cases. To evaluate the accuracy of our approach, we computed the maximum phase error ($\theta_{s,err} = |\hat{\theta}_{S_j} - \theta_{S_j}|$). As seen from Table 1, the maximum phase error computed by OSCR is $\theta_{s,err} = 1.9^0$. But this error is mostly attributed to system hardware component non-idealities. Therefore, this error can be removed via calibration.

It can be concluded that the on-site coding receiver was able to perform digital beamforming with a minimal phase error after employing onsite coding/decoding.

Table 1. Angle Estimation for dual band 8-channel OSCR

Cases	Incident Angle		Measured Angle		Maximum Error
	θ_{S_1}	θ_{S_2}	$\hat{\theta}_{S_1}$	$\hat{\theta}_{S_2}$	$\theta_{s,err}$
1.	0^0	50^0	0^0	50^0	$\mathbf{0^0}$
2.	-10^0	40^0	-9.8^0	41.8^0	$\mathbf{1.8^0}$
3.	-20^0	30^0	-19.6^0	31.4^0	$\mathbf{1.2^0}$
4.	-30^0	20^0	-29.1^0	20.4^0	$\mathbf{0.9^0}$
5.	-40^0	10^0	-39.1^0	10.4^0	$\mathbf{1.9^0}$

6. Conclusion

We presented a dual band multi-channel experimental validation of the novel on-site coding receiver system using an UWB antenna array. Specifically, we used COTS components, in-house fabrication PCBs, and FPGA to build the system and carry out its verification. Measurements were performed in the anechoic chamber to verify and validate phase recovery and estimate angel of arrival. These measurements showed that on-site coding has very minimal effect on phase error and SNR degradation when 8-chanels are combined. Concurrently, servicing of 8-channels using one ADC led to 85% reduction in power and 80% cost reduction. We remark that a key advantage of OSCR is its multi-band capability attractive for multiple input multiple output (MIMO) systems.

7. References

1. I. Tzanidis, K. Sertel, and J. L. Volakis, “Interwoven spiral array (ISPA) with a 10:1 bandwidth on a ground plane,” IEEE Antennas Wireless Propagation Letter, vol. 10, pp. 115–118, Mar. 2011.

2. W. F. Moulder, K. Sertel, J. L. Volakis, "Superstrate-Enhanced Ultrawideband Tightly Coupled Array With Resistive FSS," IEEE Transactions on Antennas and Propagation , vol. 60, no. 9, pp. 4166-4172, 2012.

3. J. P. Doane, K. Sertel, and J. L.Volakis,, "A Wideband, Wide Scanning Tightly Coupled Dipole Array with Integrated Balun (TCDA-IB)," IEEE Trans. Antenna Propagation, vol. 61 , no. 9, pp. 4538-4548, 2013.

4. D. Papantonis and J. L. Volakis, “Dual polarized tightly coupled array with substrate loading,” IEEE Antennas and Wireless Propagation Letters, vol. PP, no. 99, pp. 1–1, 2015.

5. N. Nahar, B. Raines, R. Rojas and B. Strojny, "Wideband antenna arary beam steering with free-space optical true-time delay engine," Microwaves, Antennas Propagation, IET, vol. 5, no. 6, pp. 740-746, 2011

6. R. Miura, T. Tanaka, I. Chiba, A. Horie, and Y. Karasawa, “Beamforming experiment with a DBF multibeam antenna in a mobile satellite environment,” IEEE Transactions on Antennas and Propagation, vol. 45, no. 4, pp. 707–714, Apr 1997

7. J. Fredrick, Y. Wang, S. S. Jeon and T. Itoh, "Smart antennas based on spatial multiplexing of local elements (SMILE) for mutual coupling reduction," IEEE Transactions on Antennas and Propagation, vol. 52, no. 1, pp. 106-114, 2004.

8. A. Jahanian, F. Tzeng and P. Heydari, "Code-modulated path-sharing multi-antenna receivers: theory and analysis," IEEE Transactions on Wireless Communications, vol. 8, no. 5, pp. 2193-2201, 2009.

9. Alwan EA, Balasubramanian S, Atallah JG, LaRue M, Sertel K, Khalil W, Volakis JL., "Coding-based ultra-wideband digital beamformer with significant hardware reduction.," Analog Integrated Circuits and Signal Processing, vol. 78, no. 3, p. 691–703, Mar 2013.

10. E. A. Alwan, W. Khalil and J. L. Volakis, "Low cost, power efficient, on-site coding receiver (OSCR) for ultra-wideband digital beamforming," 2013 IEEE International Symposium on Phased Array Systems and Rechnology, Boston, MA, 2013.

11. E. A. Alwan, S. B. Venkatakrishnan, A. Akhiyat, W. Khalil and J. L. Volakis, "Phase error evaluation in a two-path receiver front-end with on-site coding," IEEE Access, vol. 3, pp. 55-63, 2015.

12. S. B. Venkatakrishnan and A. A. Akhiyat and E. A. Alwan and J. L. Volakis, “Dual-band validation of on-site coding receiver using ultra-wideband antenna array at C, X and Ku-bands,” in 2016 IEEE International Symposium on Antennas and Propagation (APSURSI), June 2016, pp. 1655–1656.